

Persistent currents in rings of ultracold fermionic atoms

Yanping Cai, Daniel G. Allman, Parth Sabharwal, and Kevin C. Wright*
*Department of Physics and Astronomy, Dartmouth College,
 6127 Wilder Laboratory, Hanover NH 03766, USA*

We have produced persistent currents of ultracold fermionic atoms trapped in a toroidal geometry with lifetimes greater than 10 seconds in the strongly-interacting limit. These currents remain stable well into the BCS limit at sufficiently low temperature. We drive a circulating BCS superfluid into the normal phase and back by changing the interaction strength and find that the probability for quantized superflow to reappear is remarkably insensitive to the time spent in the normal phase and the minimum interaction strength. After ruling out the Kibble-Zurek mechanism for our experimental conditions, we argue that the reappearance of superflow is due to long-lived normal currents and the Hess-Fairbank effect.

Coherent quantum systems can support currents that remain constant in time without being driven by any external power source. These remarkable “persistent” currents may occur as metastable non-equilibrium states in superconducting [1] and superfluid [2] phases, but equilibrium persistent currents also occur in normal conducting phases around closed paths shorter than the coherence length [3–5]. Progress in understanding transport phenomena in quantum fluids has often been made by considering spherical, cylindrical, toroidal, or more exotic geometries [6], and realizing experimentally viable quantum many-body systems in more exotic geometries is an important challenge in quantum engineering. Persistent currents have been observed in experiments with Bose-Einstein condensates (BECs) of ultracold atoms [7–9], quantized phase slips [10] have been observed in matter-wave “circuits” with Josephson junctions [11, 12], and ring-BECs have been used to explore other phenomena such as collective-mode precession [13], spontaneous [14] and quench-induced currents [15], and the stability of supersonic flows [16, 17]. These previous experiments all used bosonic atoms with weak contact interactions.

In this Letter we report the creation of currents around a mesoscopic ring of ultracold fermionic atoms under conditions where they are long-lived over the entire BEC-BCS crossover. One important feature of these new experiments with superfluid rings is that we can reversibly drive the system across the superfluid phase transition by changing the interaction strength. With only a few thousand low-mass atoms under tight transverse confinement, fluctuations are much more important in these experiments than in prior work with superfluid “circuits” of heavier bosonic atoms.

A complete description of the experimental apparatus will be published separately. The experiment begins with laser cooling ${}^6\text{Li}$ atoms in a magneto-optical trap, followed by evaporative cooling to $30\ \mu\text{K}$ in a crossed-beam optical dipole trap. A movable dipole beam then transports 10^6 atoms to a glass cell between vertically oriented confocal objective lenses used for projection and imaging. We prepare the atoms in an equal mixture of the two lowest-energy spin states, which have a Feshbach

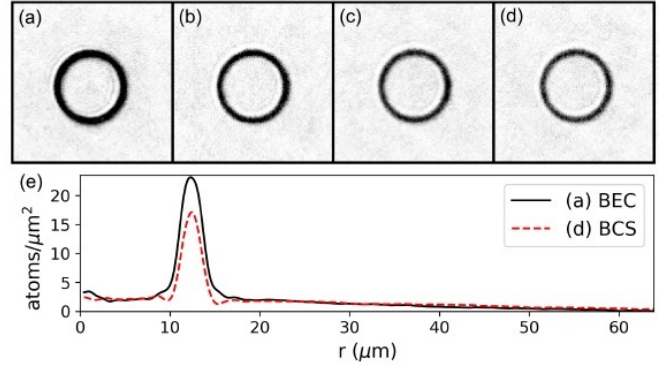


FIG. 1. Column density distribution for an equal spin mixture of $1.2(1) \times 10^4$ ${}^6\text{Li}$ atoms in a ring-dimple trap, which changes when the interactions are tuned from the (a) BEC limit to the (d) BCS limit using a Feshbach resonance at 83.2 mT. The magnetic field and scattering length for each image are: (a) $B = 68.3$ mT, $a = 68.3$ nm (b) $B = 85.7$ mT, $a = -970$ nm (c) $B = 98.0$ mT, $a = -236$ nm (d) $B = 107.8$ mT, $a = -179$ nm. Each image is an average of 10 experimental runs. The field of view is $29\ \mu\text{m} \times 29\ \mu\text{m}$. (e) Azimuthally averaged column density from (a) and (d) showing the difference between the BEC limit (dashed line) and the BCS limit (solid line). The chemical potential is higher in the BCS limit, causing more atoms to occupy states outside the ring-dimple.

resonance at a magnetic field of 83.2 mT. The atoms undergo final cooling to degeneracy in an optical trap with a ring-shaped potential minimum of radius $R = 12.0(1)\ \mu\text{m}$ [18] in a uniform 82 mT magnetic field, after which there are $N = 1.2(1) \times 10^4$ atoms paired into weakly bound ${}^6\text{Li}_2$ molecules with strong repulsive interactions.

Figure 1 shows the changing distribution of atoms in the trap when the interactions are tuned between the BEC and BCS limits. In the weakly-interacting molecular BEC (mBEC) limit at 68.3 mT, shown in Fig. 1(a), the fraction of molecules in the spatial region of the ring-dimple is 0.38(2). The remainder form a broad halo more readily seen in the plot of azimuthally averaged column density (black line) shown in Fig. 1(e). In the (weakly-attractive) BCS limit, shown in Fig. 1(d), the increase of the chemical potential to the Fermi energy (E_F) reduces

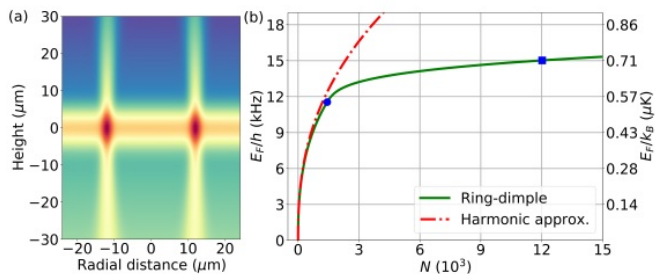


FIG. 2. (a) Vertical cross-section of a model of the trapping potential. The model includes the potentials of the horizontal sheet beam, the vertical ring beam, and gravity. The total trap depth is $2.6 \mu\text{K}$ (for molecules). (b) Calculated Fermi energy (E_F) versus total atom number N for an equal spin mixture of ${}^6\text{Li}$ atoms in the trapping potential shown in (a). The circle at $N \approx 1500$ marks the ring-dimple capacity, above which atoms occupy states extending into the broad, flat region of the trap potential due to the sheet beam alone. The square marks the atom number used in the experiment and corresponding Fermi energy. The dash-dotted line (red on-line) shows $E_F(N)$ for a 3D harmonic approximation of the ring potential minimum, for comparison.

the fraction of atoms in the ring-dimple spatial region to $0.25(2)$, with the balance moving to the halo as shown by the dashed line in Fig. 1(e).

Fig. 2(a) is a vertical cross-section through a model of the trapping potential, which is formed by the intersection of two red-detuned beams: a horizontal “sheet” beam and a vertical ring-pattern beam [8]. The trap depth for molecules is $2.6 \mu\text{K}$ ($1.5 \mu\text{K}$ from the sheet beam, and $1.1 \mu\text{K}$ from the ring beam). The vertical (radial) trapping frequency for atoms near the minimum of the ring-dimple is $\omega_z = 2\pi \cdot 1.5(1) \times 10^3 \text{ s}^{-1}$ ($\omega_r = 2\pi \cdot 4.0(2) \times 10^3 \text{ s}^{-1}$); the ring is more tube-like than disk-like. There is a 10% rms variation in density around the ring (from minor imperfections in the beams) which is stable from shot to shot.

The fraction of atoms energetically confined to the ring-dimple region in the BCS limit can be estimated by computing the semiclassical density of states and integrating to obtain $E_F(N)$. In Figure. 2(b) there is a clear “knee” in the plot of $E_F(N)$ beginning at $N = 1500$, indicated by the circle. For larger N , atoms occupy halo states that are less localized. For the experimental value of $N = 1.2 \times 10^4$ atoms the model predicts $E_F = h \cdot 15.0(2) \text{ kHz} = k_B \cdot 0.72(1) \mu\text{K}$ and a peak 3D density of $\rho = 2.6(2) \text{ atoms}/\mu\text{m}^3$. This estimate is consistent with the peak vertical column density in Fig. 1(d), after we account for the trap profile in the vertical direction and the $1.4 \mu\text{m}$ resolution limit of the imaging system.

We monitor the temperature of the system during evaporation by measuring the vertical expansion of molecules in the halo when the trap is shut off [19]. Our data indicate a final temperature of $T = 0.07(2) \mu\text{K}$ in the BEC limit, well below the temperature for formation

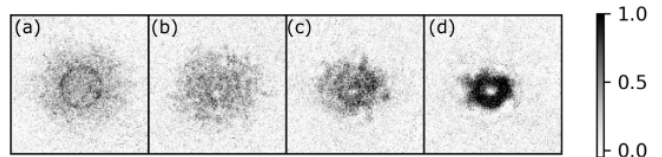


FIG. 3. Absorption images showing the cloud evolution after release from the optical trap, in the presence of a weak radial magnetic field gradient. Each image is a different realization of the experiment. (a) The cloud in the trap after the ring confinement has been relaxed and the magnetic field has been swept from 82 mT to 68.3 mT to lower the interaction energy. (b)-(d) Evolution of the density profile for 5.5 ms after the trap is shut off. Radial magnetic lensing improves the signal-to-noise ratio in detecting the vortex core associated with the persistent current. The scale at right is optical depth. The field of view of each image is $63 \mu\text{m} \times 63 \mu\text{m}$.

of a condensate at the ring minimum ($\approx 0.2 \mu\text{K}$). There is a high probability ($>50\%$) of spontaneous currents appearing during formation of the mBEC, so to initialize the current state we use a repulsive potential that can be moved in the plane of the ring. This repulsive potential is created by a steerable blue-detuned ($\lambda = 635 \text{ nm}$) beam with a focal diameter larger than the ring width (to reduce alignment sensitivity). We initialize the system in a zero-current state (winding number $\ell = 0$) by keeping the beam stationary at one point on the ring, increasing the repulsive potential linearly over 100 ms until the peak is well above the chemical potential, holding for 100 ms , then ramping the beam off in 100 ms . After this initialization procedure the probability of detecting a non-zero current ($P_{\ell \neq 0}$) is $0.00^{+0.02}_{-0.00}$ [20, 21].

To create a non-zero current state ($\ell \neq 0$), we ramp up and hold the beam power as described above, then we accelerate the focal spot azimuthally around the ring at 100 rad/s^2 up to an angular velocity that we hold constant for 300 ms , with the beam power ramping off linearly in the final 100 ms . The angular frequency of a quantized current of pairs with winding number ℓ in our ring is $\ell\Omega_0 \equiv \ell\hbar/(m_{\text{pair}}R^2) = 2\pi\ell \cdot 5.83(2) \text{ s}^{-1}$. The probability of creating an $\ell = 1$ current state ($P_{\ell=1}$) becomes measurably different from zero for stirring frequencies near $0.5 \Omega_0$ and increases to $1.00^{+0.00}_{-0.02}$ around $0.7 \Omega_0$. We can create current states with $\ell > 1$ by stirring at higher angular velocities, but in this work we focus on creation and decay of the $\ell = 1$ current state.

We detect quantized currents in the superfluid ring by releasing it from the trap and observing the density dip that appears at the phase singularity in the order parameter as it expands (See Fig. 3). The appearance of this vortex-like feature depends on the details of the expansion dynamics [22] and the interaction strength. This feature is most visible in the weakly-interacting mBEC limit. Stronger interactions cause the cloud to expand

more rapidly and can prevent detection if the density drops too low before the vortex feature grows to an optically resolvable size. When we release a BCS superfluid directly from the ring no density dip appears because the pairs break and the expansion is incoherent for $T > 0$.

We use the following multi-step detection process to improve the sensitivity of our current detection procedure: With the interactions tuned near resonance we relax the radial confinement by lowering the ring beam power by 95% over 100 ms. This causes the density profile to adiabatically change from the narrow ring shown in Fig. 1 to the profile shown in Fig. 3(a), where the density at the center of the cloud is clearly non-zero. If a current was present in the superfluid ring there will be a vortex in this central region, with a core size below the optical resolution limit. We maintain an above-average density in the ring-dimple region to keep the vortex trapped near the center of the cloud while we sweep the magnetic field from $B_i = 82$ mT to $B_f = 68.3$ mT in 20 ms, reducing the scattering length by 96%. Finally, we turn off the optical trap diabatically and allow the system to evolve for 5.5 ms before absorption imaging on the cycling transition $|m_J = -1/2, m_I = 1\rangle \rightarrow |m_J = -3/2, m_I = 1\rangle$. Radial curvature in the magnetic bias field causes 2D focusing of the cloud, and the momentum state before release can be determined from the density distribution in the final image [23, 24], as shown in Fig. 3(d).

We have confirmed that persistent currents survive for at least 10 seconds in the strongly interacting limit, given our vacuum-limited trap lifetime is around 12 seconds. As the total number of atoms decreases, we observe larger density fluctuations in the time-of-flight images. For $N < 6 \times 10^3$ we cannot distinguish a vortex from the fluctuations with the technique described above. We expect to achieve greater sensitivity for low atom numbers in future experiments by adapting interferometric techniques previously demonstrated with bosonic superfluids [12].

In the BCS limit the current becomes increasingly fragile, with T_c decreasing exponentially as the interaction strength becomes weaker. To find the threshold for decay of the current in the BCS regime we first prepare the system in the strongly-interacting mBEC regime at $B_i = 82$ mT, then sweep the magnetic field across the entire Feshbach resonance in 100 ms to a value B_{\max} on the BCS side of resonance, and finally sweep it back to B_i in 100 ms before measuring the current. The 100 ms sweep time is slow enough that the change in density profile shown in Fig. 1 is adiabatic and does not excite collective modes in the ring.

We found that the current did not decay during this procedure for ramps with $B_{\max} \leq 98$ mT ($1/k_F a \leq -1.00$). Survival of the current in the BCS regime is only possible if the system temperature is very low. For a uniform 3D Fermi gas in the BCS limit, the predicted superfluid critical temperature is $T_c \approx 0.277 T_F e^{-\pi/2k_F |a|}$,

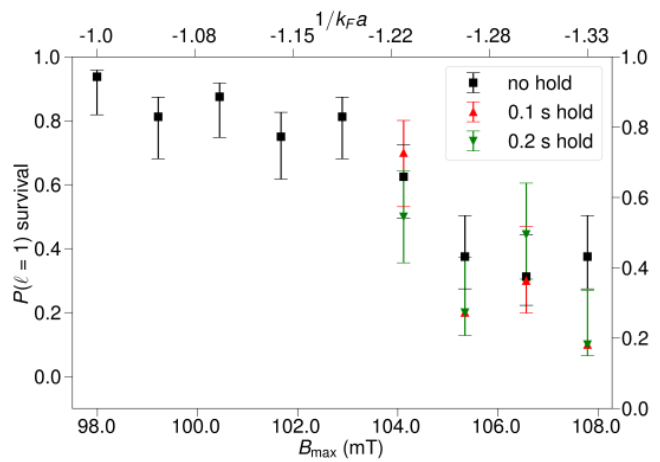


FIG. 4. Probability of detecting an $\ell = 1$ current after preparing a ring-mBEC in that state, then ramping the interactions into the BCS regime and back. The probability is plotted as a function of the maximum magnetic field (B_{\max}) used in the ramp (lower scale) and the interaction parameter $1/k_F a$ (upper scale), where a is the scattering length and $2\pi/k_F = 1.49 \mu\text{m}$ is the Fermi wavelength). Black squares are averaged data from 16 runs each where B was ramped up from 82 mT and back down with no hold time at B_{\max} . Triangles shown for the 4 highest values of B_{\max} are averaged data from 10 runs each and a hold time at B_{\max} of 0.1 s (upright, red online) or 0.2 s (inverted, green online).

where k_F is the Fermi wavenumber and a is the scattering length [25]. For the average value of the peak density around the ring, this gives $T_c = 32$ nK at $1/k_F a = -1.00$. This prediction is consistent with the cooling that is expected to occur when adiabatically ramping from the BEC to BCS regime [26], but should be considered an upper bound on T_c because it does not account for increased fluctuations caused by the tight transverse confinement of the atoms to the ring.

Figure 4 shows the decreasing probability of detecting an $\ell = 1$ current ($P_{\ell=1}$) as B_{\max} increases from 98 mT to our technical limit of 107.8 mT. The decrease of $P_{\ell=1}$ from unity over the range from 98 mT to 103 mT in Fig. 4 is likely due to thermally activated phase slips, since $k_B T$ is much larger than the kinetic energy of the pairs. The flow velocity for an $\ell = 1$ supercurrent is 0.44 mm/s, which is small compared to the Fermi velocity ($v_F = 45$ mm/s) and sound velocity ($0.25\text{-}0.5 v_F$ [27]). The sudden drop in $P_{\ell=1}$ around 104 mT ($1/k_F a = -1.22$) likely indicates that $T_c \approx T$ at that point. Using the local density approximation $T_c = 26$ nK for those conditions, but we reiterate that this is an upper bound and a more careful calculation is needed.

For even higher magnetic fields $T > T_c$, the superfluid vanishes, and any angular momentum initially carried by it must be somehow transferred to the normal fluid. For $1/k_F a$ in this range the gas is nearly collisionless, and the lifetime of the normal current should depend on tem-

perature and the disorder in the potential. If the current lifetime is short compared to the time spent in the normal phase near B_{\max} , $P_{\ell=1}$ should fall to zero. Instead, for $B_{\max} \geq 105$ mT, $P_{\ell=1}$ was consistently around 0.3. $P_{\ell=1}$ also did not decrease significantly after adding hold times of up to 200 ms at B_{\max} (see Fig. 4), indicating negligible damping of the normal current on this timescale. Damping times on the order of a second have been observed in unitary Fermi gases in the hydrodynamic limit [28], and while increased damping has been observed for intermediate values of $1/k_F a$ and $T/T_c \approx 1$ [29], our system is far enough into the collisionless limit and the temperature is low enough that a damping time of 0.5 second or more is plausible.

Before we can be confident that the normal current is long-lived, we must rule out the competing possibility that the normal current does decay and the currents we observe after returning to the superfluid phase are generated spontaneously via the Kibble-Zurek mechanism [30]. To test this hypothesis we prepared the atoms in the $\ell = 0$ state and measured the probability of observing a non-zero current after similarly ramping the magnetic field to the BCS limit and back. The probability of observing a spontaneous current under those ramp conditions was $0.04_{-0.01}^{+0.08}$, which indicates that this mechanism is not important for the data shown in Fig. 4.

We next address the reason why $P_{\ell=1}$ levels off at a value of 0.3 when the system is driven fully normal and back to the superfluid phase. When a normal fluid subjected to a nonzero rotational “flux” is driven into the superfluid phase, it will form a quantized supercurrent with a winding number that minimizes the free energy. If the normal fluid in our system is rotating with some angular velocity Ω_n (where $0 < \Omega_n < \Omega_0$), and phase fluctuations are small, the superfluid ring should re-form in the $\ell = 0$ state for $\Omega_n < \Omega_0/2$, and in the $\ell = 1$ state for $\Omega_n > \Omega_0/2$. This “rotational Meissner effect” was first seen in liquid helium in a rotating container by Hess and Fairbank [31], and has more recently been observed in ultracold atoms subjected to a flux from a synthetic gauge potential [32].

In our system phase fluctuations are likely large enough to broaden the distribution of final current states for a given Ω_n . If $P_{\ell=1}$ is closer to a linear function of Ω_n , then a value of Ω_n between 0.3 and $0.5 \omega_0$ would be consistent with the observation that $P_{\ell=1} = 0.3$ for $B_{\max} > 105$ mT. When we create the $\ell = 1$ supercurrent in the ring, the superfluid fraction is around 1/3. This would lead to a normal current in the specified range as long as the damping time for the normal current is sufficiently long.

In conclusion, we have studied persistent currents in a fermionic quantum gas confined in a toroidal geometry in the regime of strong interactions and in the BCS limit of weak attraction. We have achieved conditions where supercurrents remain metastable well into the BCS limit, and the normal current damping time is long enough to

observe the Hess-Fairbank effect. These studies of persistent currents in a spin-balanced Fermi gas in a 3D ring provide a foundation for further studies of transport and non-equilibrium phenomena in rings of ultracold fermionic atoms. In these experiments we confirmed that spontaneous currents do not appear for slow enough interaction ramps across the superfluid transition. However, we have seen spontaneous currents appear after faster ramps. This presents an exciting opportunity to study the Kibble-Zurek mechanism with fermions [33] in the annular geometry originally proposed by Zurek [34]. These experiments were conducted with an unpolarized Fermi gas in a ring, but a weakly polarized gas could enable the creation of matter-wave circuits with π -Josephson junctions [35] and provide a new opportunity to search for exotic spin-polarized superfluid phases [36, 37]. Finally, the tight transverse confinement achieved in these experiments is not far from the quasi-1D limit, and it may be feasible to create 1D quantum rings [38] of fermions with tunable interactions, where non-Fermi-liquid behavior is expected and parity effects can be significant [39].

We thank J. Evans, S. Khatry, L. Bezerra, and A. Woronecki for key technical contributions to the experimental apparatus and recognize D. Adams, C. Grant, and D. Collins for critical engineering support. We also thank R. Onofrio for insightful discussions about ultracold fermionic systems. This work was supported by the NSF (Grant No. PHY-1707557).

* Kevin.Wright@Dartmouth.edu

- [1] B. S. Deaver and W. M. Fairbank, Experimental evidence for quantized flux in superconducting cylinders, *Phys. Rev. Lett.* **7**, 43 (1961).
- [2] P. P. J. Bendt, Superfluid Helium Critical Velocities in a Rotating Annulus, *Phys. Rev.* **127**, 1441 (1962).
- [3] M. Büttiker, Y. Imry, and R. Landauer, Josephson behavior in small normal one-dimensional rings, *Phys. Lett. A* **96**, 365 (1983).
- [4] H. Bluhm, N. C. Koshnick, J. A. Bert, M. E. Huber, and K. A. Moler, Persistent Currents in Normal Metal Rings, *Phys. Rev. Lett.* **102**, 136802 (2009).
- [5] A. C. Bleszynski-Jayich, W. E. Shanks, B. Peaudecerf, E. Ginossar, F. von Oppen, L. Glazman, and J. G. E. Harris, Persistent Currents in Normal Metal Rings, *Science* **326**, 272 (2009).
- [6] E. Fradkin, *Field Theories of Condensed Matter Physics* (Cambridge University Press, Cambridge, 2013).
- [7] C. Ryu, M. F. Andersen, P. Cladé, V. Natarajan, K. Helmerson, and W. D. Phillips, Observation of Persistent Flow of a Bose-Einstein Condensate in a Toroidal Trap, *Phys. Rev. Lett.* **99**, 260401 (2007).
- [8] A. Ramanathan, K. C. Wright, S. R. Muniz, M. Zelan, W. T. Hill, C. J. Lobb, K. Helmerson, W. D. Phillips, and G. K. Campbell, Superflow in a Toroidal Bose-Einstein Condensate: An Atom Circuit with a Tunable Weak

- Link, *Phys. Rev. Lett.* **106**, 130401 (2011).
- [9] S. Beattie, S. Moulder, R. J. Fletcher, and Z. Hadzibabic, Persistent Currents in Spinor Condensates, *Phys. Rev. Lett.* **110**, 025301 (2013).
- [10] K. C. Wright, R. B. Blakestad, C. J. Lobb, W. D. Phillips, and G. K. Campbell, Driving Phase Slips in a Superfluid Atom Circuit with a Rotating Weak Link, *Phys. Rev. Lett.* **110**, 025302 (2013).
- [11] C. Ryu, P. W. Blackburn, A. A. Blinova, and M. G. Boshier, Experimental Realization of Josephson Junctions for an Atom SQUID, *Phys. Rev. Lett.* **111**, 205301 (2013).
- [12] S. Eckel, F. Jendrzejewski, A. Kumar, C. J. Lobb, and G. K. Campbell, Interferometric Measurement of the Current-Phase Relationship of a Superfluid Weak Link, *Phys. Rev. X* **4**, 031052 (2014).
- [13] G. E. Marti, R. Olf, and D. M. Stamper-Kurn, Collective excitation interferometry with a toroidal Bose-Einstein condensate, *Phys. Rev. A* **91**, 013602 (2015).
- [14] C. N. Weiler, T. W. Neely, D. R. Scherer, A. S. Bradley, M. J. Davis, and B. P. Anderson, Spontaneous vortices in the formation of Bose-Einstein condensates, *Nature* **455**, 948 (2008).
- [15] L. Corman, L. Chomaz, T. Bienaimé, R. Desbuquois, C. Weitenberg, S. Nascimbène, J. Dalibard, and J. Beugnon, Quench-induced supercurrents in an annular Bose gas, *Phys. Rev. Lett.* **113**, 135302 (2014).
- [16] S. Pandey, H. Mas, G. Drougakis, P. Thekkeppatt, V. Bolpasi, G. Vasilakis, K. Poulios, and W. von Klitzing, Hypersonic Bose-Einstein condensates in accelerator rings, *Nature* **570**, 205 (2019).
- [17] Y. Guo, R. Dubessy, M. d. G. de Herve, A. Kumar, T. Badr, A. Perrin, L. Longchambon, and H. Perrin, Supersonic Rotation of a Superfluid: A Long-Lived Dynamical Ring, *Phys. Rev. Lett.* **124**, 025301 (2020).
- [18] Uncertainties are the uncorrelated combination of 1σ statistical and systematic uncertainties unless stated otherwise.
- [19] Expansion caused by weak magnetic anti-trapping in the vertical direction is negligible compared to the measurement uncertainty.
- [20] Uncertainties in average measured winding number are estimated following the Bayesian approach of Ref [21].
- [21] E. Cameron, On the Estimation of Confidence Intervals for Binomial Population Proportions in Astronomy: The Simplicity and Superiority of the Bayesian Approach, *Pub. Astr. Soc. Australia* **28**, 128 (2011).
- [22] N. Murray, M. Krygier, M. Edwards, K. C. Wright, G. K. Campbell, and C. W. Clark, Probing the circulation of ring-shaped Bose-Einstein condensates, *Phys. Rev. A* **88**, 053615 (2013).
- [23] I. Shvarchuck, C. Buggle, D. S. Petrov, K. Dieckmann, M. Zielonkowski, M. Kemmann, T. G. Tiecke, W. von Klitzing, G. V. Shlyapnikov, and J. T. M. Walraven, Bose-Einstein Condensation into Nonequilibrium States Studied by Condensate Focusing, *Phys. Rev. Lett.* **89**, 270404 (2002).
- [24] S. Tung, G. Lamporesi, D. Lobser, L. Xia, and E. A. Cornell, Observation of the Presuperfluid Regime in a Two-Dimensional Bose Gas, *Phys. Rev. Lett.* **105**, 230408 (2010).
- [25] L. P. Gor'kov and T. K. Melik-Barkhudarov, Contribution to the Theory of Superfluidity in an Imperfect Fermi Gas, *Sov. Phys. JETP* **13**, 1018 (1961).
- [26] L. D. Carr, G. V. Shlyapnikov, and Y. Castin, Achieving a BCS transition in an atomic Fermi gas, *Phys. Rev. Lett.* **92**, 150404 (2004).
- [27] W. Weimer, K. Morgener, V. P. Singh, J. Siegl, K. Hueck, N. Luick, L. Mathey, and H. Moritz, Critical Velocity in the BEC-BCS Crossover, *Phys. Rev. Lett.* **114**, 095301 (2015).
- [28] S. Riedl, E. R. S. Guajardo, C. Kohstall, J. H. Denschlag, and R. Grimm, Lifetime of angular momentum in a rotating strongly interacting Fermi gas, *Phys. Rev. A* **79**, 053628 (2009).
- [29] M. J. Wright, S. Riedl, A. Altmeyer, C. Kohstall, E. R. S. Guajardo, J. H. Denschlag, and R. Grimm, Finite-temperature collective dynamics of a fermi gas in the bec-bcs crossover, *Phys. Rev. Lett.* **99**, 150403 (2007).
- [30] A. Das, J. Sabbatini, and W. H. Zurek, Winding up superfluid in a torus via Bose Einstein condensation., *Sci. Rep.* **2**, 352 (2012).
- [31] G. B. Hess and W. M. Fairbank, Measurements of angular momentum in superfluid helium, *Phys. Rev. Lett.* **19**, 216 (1967).
- [32] P. K. Chen, L. R. Liu, M. J. Tsai, N. C. Chiu, Y. Kawaguchi, S. K. Yip, M. S. Chang, and Y. J. Lin, Rotating Atomic Quantum Gases with Light-Induced Azimuthal Gauge Potentials and the Observation of the Hess-Fairbank Effect, *Phys. Rev. Lett.* **121**, 250401 (2018).
- [33] B. Ko, J. W. Park, and Y. Shin, Kibble-Zurek universality in a strongly interacting Fermi superfluid, *Nature Physics* **15**, 1227 (2019), 1406.4073.
- [34] W. H. Zurek, Cosmological experiments in superfluid helium?, *Nature* **317**, 505 (1985).
- [35] T. Kashimura, S. Tsuchiya, and Y. Ohashi, II-junction and spontaneous current state in a superfluid Fermi gas, *Phys. Rev. A* **84**, 013609 (2011).
- [36] Y.-A. Liao, A. S. C. Rittner, T. Paprotta, W. Li, G. B. Partridge, R. G. Hulet, S. K. Baur, and E. J. Mueller, Spin-imbalance in a one-dimensional Fermi gas., *Nature* **467**, 567 (2010).
- [37] Y. Yanase, Angular Fulde-Ferrell-Larkin-Ovchinnikov state in cold fermion gases in a toroidal trap, *Phys. Rev. B* **80**, 220510(R) (2009).
- [38] S. Viefers, P. Koskinen, P. Singha Deo, and M. Manninen, Quantum rings for beginners: energy spectra and persistent currents, *Physica E: Low-dimensional Systems and Nanostructures* **21**, 1 (2004).
- [39] G. Pecci, P. Naldesi, L. Amico, and A. Minguzzi, Probing the BCS-BEC crossover with persistent currents, *arXiv* , 2010.03552 (2020).